

Close Binary Progenitors of Long Gamma Ray Bursts

Maxim V. Barkov,^{1,2*} Serguei S. Komissarov^{1†}

¹*Department of Applied Mathematics, The University of Leeds, Leeds, LS2 9GT, UK*

²*Space Research Institute, 84/32 Profsoyuznaya Street, Moscow 117997, Russia*

Received/Accepted

ABSTRACT

The strong dependence of the neutrino annihilation mechanism on the mass accretion rate makes it difficult to explain the LGRBs with duration in excess of 100 seconds as well as the precursors separated from the main gamma-ray pulse by few hundreds of seconds. Even more difficult is to explain the *Swift* observations of the shallow decay phase and X-ray flares, if they indeed indicate activity of the central engine for as long as 10^4 seconds. These data suggest that some other, most likely magnetic mechanisms have to be considered. Since the efficiency of magnetic mechanisms does not depend that much on the mass accretion rate, the magnetic models do not require the development of accretion disk within the first few seconds of the stellar collapse and hence do not require very rapidly rotating stellar cores at the pre-supernova state. This widens the range of potential LGRB progenitors. In this paper, we re-examine the close binary scenario allowing for the possibility of late development of accretion disks in the collapsar model and investigate the available range of mass accretion rates, black hole masses, and spins. We find that the black hole mass can be much higher than $2 - 3M_{\odot}$, usually assumed in the collapsar model, and normally exceeds half of the pre-supernova mass. The black hole spin is rather moderate, $a = 0.4 - 0.8$, but still high enough for the Blandford-Znajek mechanism to remain efficient provided the magnetic field is sufficiently strong. Our numerical simulations confirm the possibility of magnetically driven stellar explosions, in agreement with previous studies, but point towards the required magnetic flux on the black hole horizon in excess of 10^{28}G cm^2 . At present, we cannot answer with certainty whether such a strong magnetic field can be generated in the stellar interior. Perhaps, the supernova explosions associated with LGRBs are still neutrino-driven and their gamma-ray signature is the precursors. The supernova blast clears up escape channels for the magnetically driven GRB jets, which may produce the main pulse. In this scenario, the requirements on the magnetic field strength can be lowered. A particularly interesting version of the binary progenitor involves merger of a WR star with an ultra-compact companion, neutron star or black hole. In this case we expect the formation of very long-lived accretion disks, that may explain the phase of shallow decay and X-ray flares observed by *Swift*. Similarly long-lived magnetic central engines are expected in the current single star models of LGRB progenitors due to their assumed exceptionally fast rotation.

Key words: black hole physics – accretion disks – supernovae: general – gamma-rays: bursts – binaries: close – MHD – relativity

1 INTRODUCTION

The nature of Gamma Ray Bursts (GRBs) remains one of the most intriguing problems of modern astrophysics. It is now widely accepted that the gamma ray emission is generated in ultrarelativistic jets but many basic questions related both to the physics of these jets and to the mechanisms

of their production remain open. Although many promising theories have been developed over the years since the discovery of GRBs, we are still some way out from solid understanding of this phenomenon. For example, the observed connection between the Long-duration Gamma Ray Bursts (LGRBs) and supernovae (SNe) indicates that these bursts are connected to deaths of massive stars but the details are not clear. In one model of LGRBs, the stellar collapse results in a normal successful supernova explosion but the newly born neutron star (NS) is very unusual. It

* E-Mail: bmv@maths.leeds.ac.uk

† E-Mail: serguei@maths.leeds.ac.uk

has both exceptionally high magnetic field, and for this reason it is called a magnetar, and extremely rapid rotation (e.g. Usov 1992; Thompson et al. 2004; Metzger et al. 2007; Uzdensky & MacFadyen 2007). The powerful magnetohydrodynamic (MHD) wind produced by such remnant is capable of both accelerating the supernova shell above the expansion speed of normal supernovae, to the level of hypernovae, and production of collimated ultra-relativistic polar jets (Komissarov & Barkov 2007; Bucciantini et al. 2009).

In another model, the normal supernova explosion fails and the proto-neutron star promptly collapses into a black hole (BH). However, the rapid rotation of the stellar progenitor prevents the rest of the star from falling directly into the black hole and a massive neutrino-cooled accretion disk is formed instead. This allows to turn the failed supernova into a successful stellar explosion, as this disk can release enormous amounts of energy (Woosley 1993; MacFadyen & Woosley 1999). One way of “utilising” this energy is via the neutrino- or magnetically-driven wind from the disk. Such wind is not expected to be relativistic due to the high mass loading at its base. However, the polar region just above the black hole is less likely to become mass-loaded by the disk matter and can become relativistically hot via annihilation of neutrinos and anti-neutrinos emitted by the disk. This opens a possibility of driving ultra-relativistic LGRB jets in the collapsar scenario (e.g. MacFadyen & Woosley 1999; Aloy et al. 2000). However, the efficiency of this type of neutrino heating is a very strong function of both the mass accretion rate and the rotation rate of the central black hole (Popham et al. 1999; Chen & Beloborodov 2007; Zalamea & Beloborodov 2009). According to the calculations by Popham et al. (1999) for the black hole with the rotation parameter $a = 0.5$ the energy deposition rate via the neutrino annihilation process drops from $L_{\nu\bar{\nu}} = 4 \times 10^{48}$ erg/s for $\dot{M} = 0.1M_{\odot}$ to $L_{\nu\bar{\nu}} = 6 \times 10^{44}$ erg/s for $\dot{M} = 0.01M_{\odot}$ and for the accretion rate of $\dot{M} = 0.1M_{\odot}$ from $L_{\nu\bar{\nu}} = 2 \times 10^{51}$ erg/s for $a = 0.95$ to $L_{\nu\bar{\nu}} = 3 \times 10^{48}$ erg/s for $a = 0$. Therefore, this version of the collapsar model, similarly to the magnetar model, requires very rapid rotation of the stellar core prior to the collapse so that the accretion disk is formed early on, when the accretion rate is still high enough, and the BH is born rapidly rotating. The results by Birkel et al. (2007) suggest that Popham et al. (1999) may have overestimated the efficiency of neutrino mechanism for high a . This is because the energy released by the disk powers not only the outflow but also the flow into the BH. As a increases the inner boundary of the disk moves closer to the BH and a larger fraction of the total neutrino-antineutrino annihilation occurs in the region where the vector of deposited momentum points towards the black hole. In fact, Birkel et al. (2007) find that the efficiency of the neutrino annihilation mechanism peaks at $a \simeq 0.6$.

It turns out that such a fast rotation cannot be a general result of stellar evolution. Although young massive star often rotate sufficiently rapidly at birth, their cores are expected to experience strong spin-down during the red giant phase and during the intensive mass loss period characteristic for massive stars at the Wolf-Rayet phase (Heger et al. 2005). In fact, this theoretical result agrees very well with the observed rotation rates of newly born pulsars. Thus in order to retain the rotation rate required in the collapsar model,

the evolution of LGRB progenitors must proceed along a rather exotic route. Recently, it was proposed that a combination of low metallicity and extremely fast initial rotation, at around 50% of the break-up speed, could lead to such a route (Yoon & Langer 2005; Woosley & Heger 2006; Yoon et al. 2006). On one hand, the mass-loss rate decreases significantly with metallicity, leading to a significant reduction in the total loss of angular momentum. On the other hand, the rotationally induced circulation becomes very effective at such a high rotation rate and may result in chemically homogeneous stars that avoid the development of extended envelopes and hence the spin-down of stellar cores via interaction with these envelopes. Moreover, the star remains compact by the time of its collapse so the LGRB jet can break out from the star on the time scale compatible with the observed durations of LGRBs.

Another exotic scenario involves close high-mass binary systems, where the fast rotation of stellar cores is sustained via the tidal interaction between companions (Tutukov & Cherepashchuk 2003, 2004; Izzart et al. 2004; Podsiadlowski et al. 2004; van den Heuvel and Yoon 2007). In this case, the pre-supernova is a compact helium star, essentially a Wolf-Rayet (WR) star, because the extended envelope is dispersed into the surrounding space during the common envelope phase. The stellar rotation in such systems is synchronised with the orbital motion on a very short time scale (e.g. van den Heuvel and Yoon 2007). The contraction of CO-cores during stellar evolution leads to their additional spin-up but due to the core-envelope coupling only a fraction of their angular momentum is retained (Yoon et al. 2006). As the result, the core rotation rate is insufficient in the cases where the companion of the helium star is a main-sequence star. According to van den Heuvel and Yoon (2007), the core rotation can be high enough to fit the collapsar model with the neutrino-driven LGRB jet only if the component is also a compact star, namely NS or BH. Three examples of such systems are known to date: Cyg X-3, IC 10 X-1, and NGC 300 X-1. Cyg X-3 has a very short orbital period, only 4.8h (van Kerkwijk et al. 1992), and the radius of the WR star in this system is less than $3 - 6R_{\odot}$ (Cherepashchuk & Mofat 1994). The recently discovered IC 10 X-1 and NGC 300 X-1 have the orbital periods of 35h and 33h respectively (Carpano et al. 2007; Prestwich et al. 2007; Silverman & Filippenko 2008). The masses of Wolf-Rayet stars are estimated at $18 - 40M_{\odot}$ for NGC 300 X-1 and $\simeq 35M_{\odot}$ for IC 10 X-1 (Clark & Crowther 2004). Given the observed production rate of such systems van den Heuvel and Yoon (2007) predicted one hypernova/LGRB every 2000 years in a galaxy similar to our own.

The neutrino heating is not the only possible mechanism behind the explosions of collapsing stars. Perhaps somewhat less popular, but the magnetic mechanisms are also regarded as potentially important (e.g. Bisnovatyi-Kogan 1970; LeBlanc & Wilson 1970; MacFadyen et al. 2001; Moiseenko et al. 2006; Burrows et al. 2007). Likewise, the LGRB jets can also be powered via a magnetic mechanism, in particular the Blandford-Znajek mechanism, which utilises the rotational energy of the BH (e.g. Blandford & Znajek 1977; Meszaros & Rees 1997; Lee et al. 2000; Proga et al. 2003; McKinney 2006; Barkov & Komissarov 2008a; Komissarov & Barkov 2009). Here the black hole is also re-

quired to rotate quite rapidly. However, the efficiency of this mechanism is not that sensitive to the mass accretion rate and such rapid rotation does not have to be achieved right after the collapse of the Fe core. Instead, it can be built up gradually during the rest of the stellar collapse. This difference in the sensitivity to mass accretion rate favours the BZ mechanism over the neutrino mechanism in the case of very long-duration LGRBs, more than 100 seconds long (MacFadyen et al. 2001). The discovery by *Swift* of the shallow decay phase and late flares in the X-ray light curves of LGRBs (Zhang 2007; Chincarini et al. 2007) also suggests that the central engine may remain active for as long as 10^4 seconds (e.g. Lipunov & Gorbovskoy 2007, 2008). Since the neutrino mechanism requires the mass accretion rate to stay above $\text{few} \times 10^{-2} M_{\odot}/\text{s}$, such a prolonged activity implies the progenitor mass in excess of $\text{few} \times 10^2 M_{\odot}$, which is highly unlikely¹.

Another problem for the model of neutrino-driven GRBs are the strong precursors sometimes observed before the arrival of the main gamma-ray pulse (Burlon et al. 2008). According to the analysis of Wang & Meszaros (2007) such precursor and the main pulse can be attributed to a single eruptive event only when the precursor and the main pulse are separated by few seconds. However, in some GRBs the delay can be as long as few hundreds of seconds and in such cases it is much more likely that the precursor and the main pulse correspond to two different events in the life of the central engine. They proposed that the precursor is produced during the supernova explosion, in the jet powered by a rotating magnetised neutron star, and that the main pulse is produced during the fallback phase when the neutron star collapses into a black hole². The typical mass accretion rates in the fallback scenario, $10^{-2} - 10^{-3} M_{\odot} \text{ s}^{-1}$, are too low for the neutrino annihilation mechanism and thus this explanation implies magnetic origin for the main pulse as well (MacFadyen et al. 2001).

Thus, the observations require to include the magnetic mechanism, either in the black hole or, in fact, in the disk version, or both, in the collapsar scenario. This widens the range of potential progenitors of LGRBs. Indeed, we no longer need to constrain ourself to the stars with extremely rapidly rotating cores but can also include the cases with slower rotation where the accretion disk forms much later during the course of stellar collapse.

In this paper we re-examine the scenario of binary progenitor of LGRBs allowing for the late formation of accretion disks and lower mass accretion rates compared to those required in the collapsar model with the neutrino mechanism. In Section 2 we determine the parameters of binary systems which allow formation of accretion disks during the collapse of WR companion. We also estimate masses and spins of the black holes by the time of accretion disk formation using simplified analytical model for the structure of pre-supernovae

¹ Typically, the mass of WR star is 9-25 M_{\odot} , though some observations suggested that it can be as high as 83 M_{\odot} (Schweickhardt et al. 1999; Crowther 2007).

² This model may struggle to explain delays shorter than the typical fallback time, 100-1000 seconds, found in one-dimensional simulations MacFadyen et al. (2001). However, due to the rotational effects the supernova explosions could be highly aspherical, resulting in shorter fallback time scales in the equatorial region.

due to Bethe (1990). In Section 3 we investigate the degree to which the black hole spin can increase later on, during the disk accretion phase, using the same approach as in the recent study by Janiuk et al. (2008). Here we consider not only the Bethe's model but also the polytropic model and the models of pre-supernovae based on detailed calculations of stellar evolution. In Section 4 we describe the numerical simulations of LGRB jet formation with setup based on the results obtained in the previous Sections. In Section 5 we analyse the potential of the binary scenario in the extreme case, which involves merger of the WR star with its ultra-compact companion, BH or NS. In Section 6 we summarise our main results and discuss their astrophysical implications.

2 FORMATION OF ACCRETION DISC

In a synchronised binary the tidal torques force the components to spin with the same rate as the orbital rotation,

$$\Omega_s^2 = GM_s(1+q)/L^3, \quad (1)$$

where L is the orbital separation, M_s is the mass of the star under consideration, and $q = M_{com}/M_s$, where M_{com} is the mass of the companion star. Since, the orbital frequency decreases with L , the maximum possible spin is reached when the separation is minimum. This corresponds to the case where the star radius is about the size of its Roche lobe. The relation between the minimum separation L_{min} , the stellar radius R_s , and q can be approximated with sufficient accuracy for $1/100 < q < 100$ as

$$L_{min} = 2.64q^{0.2084} R_s \quad (2)$$

(Plavec & Krotochvil 1964).

During the stellar collapse the centrifugal force will halt the free-fall of the outer layers and promote the development of accretion disk provided the specific angular momentum on the stellar equator exceeds that of the marginally bound circular orbit for the black hole with the same mass and angular momentum as the star. The angular momentum of Kerr black holes is

$$J_h = a \frac{GM_h^2}{c},$$

where $-1 < a < 1$ is the dimensionless spin parameter and M_h is the hole mass. The specific angular momentum of test massive particles on circular orbits in the equatorial plane is

$$l = \frac{(r^2 - 2ar^{1/2} + a^2)}{r^{3/4}(r^{3/2} - 3r^{1/2} + 2a)^{1/2}} \frac{GM_h}{c}, \quad (3)$$

where $r = R/R_g$ and $R_g = GM_h/c^2$, and the radius of the marginally bound orbit is

$$r_{mb} = \{2 - a + 2(1 - a)^{1/2}\} \quad (4)$$

(Bardeen et al. 1972). The disk formation condition is

$$\Omega_s R_s^2 > l_{mb}, \quad (5)$$

where $l_{mb} = l(r_{mb})$. As we shall see later, at the time of the disk formation a is quite small. Using the Taylor expansion we find that

$$l_{mb} = (4 - a) \frac{GM_h}{c} + O(a^2) \simeq \frac{4GM_h}{c}. \quad (6)$$

Using this result and Eq.1 we can now write the disk formation condition as

$$\left(\frac{L}{R_s}\right)^3 < \frac{1+q}{16}r_s, \quad (7)$$

where $r_s = R_s/R_{gs}$ and $R_{gs} = GM_s/c^2$. For the typical parameters of WR stars this amounts to

$$L < 14R_s(1+q)^{1/3} \left(\frac{R_s}{R_\odot}\right)^{1/3} \left(\frac{M_s}{10M_\odot}\right)^{-1/3}. \quad (8)$$

The comparison of this result with Eq.2 shows that collapse of WR stars in close binaries can indeed lead to formation of accretion discs (Bisnovatyi-Kogan & Tutukov 2004; Podsiadlowski et al. 2004). We can rewrite the above condition in terms of the binary period, T_b , as

$$T_b < \frac{1}{4}T_k r_s^{-1/2} \simeq 48\text{hr} \left(\frac{M_s}{10M_\odot}\right)^{-1} \left(\frac{R_s}{R_\odot}\right)^2, \quad (9)$$

where T_k is the Keplerian period at $R = R_s$. This upper limit is about five times higher than that obtained in Podsiadlowski et al. (2004) who required the disk to form immediately after the collapse of iron core.

Effectively cooled accretion disks remain geometrically thin and their inner radius is given by the radius of the last stable circular orbit

$$r_{ms} = \{3 + Z_2 - [(3 - Z_1)(3 + Z_1 + 2Z_2)]^{1/2}\}, \quad (10)$$

where $r_{ms} = R_{ms}/R_g$ and

$$\begin{aligned} Z_1 &\equiv 1 + (1 - a^2)^{1/3}[(1 + a)^{1/3} + (1 - a)^{1/3}], \\ Z_2 &\equiv (3a^2 + Z_1^2)^{1/2}. \end{aligned} \quad (11)$$

(Bardeen et al. 1972). The corresponding specific angular momentum, l_{ms} , determines the evolution of the black hole spin via the disk accretion³.

The outer radius of the disk, R_d , is determined by the specific angular momentum on the stellar equator⁴, $l_s = \Omega_s R_s^2$. Assuming that $r_d = R_d/R_{gs} \gg 1$ the angular momentum at the outer edge of the disk is simply

$$l_d = (GM_s R_d)^{-1/2}.$$

Matching l_d and l_s , and using Eq.1, we find that

$$r_d = r_s(1+q) \left(\frac{L}{R_s}\right)^{-3}. \quad (12)$$

Thus,

$$r_d \sim 47 \left(\frac{R_s}{R_\odot}\right) \left(\frac{M_s}{10M_\odot}\right)^{-1} \left(\frac{\tilde{L}}{10}\right)^{-3} \quad (13)$$

where $\tilde{L} = (1+q)^{-1/3}(L/R_s)$. For the widest orbital separation which still allows disk formation (see Eq.8) this equation gives $r_d \leq 17$ whereas for the closest one (see Eq.2) we have $r_d \leq 5 \times 10^3$. Thus, the model predicts a wide range of accretion disk sizes. Compact disks and the inner regions of large disks will cool via the neutrino emission, whereas

³ For simplicity, we ignore the effects of magnetic torques on the evolution of black hole spin.

⁴ In fact, various torques operating in the accretion disk change the angular momentum and hence the location of the outer edge but this effect is relatively minor (Shakura & Sunyaev 1973; Chen & Beloborodov 2007).

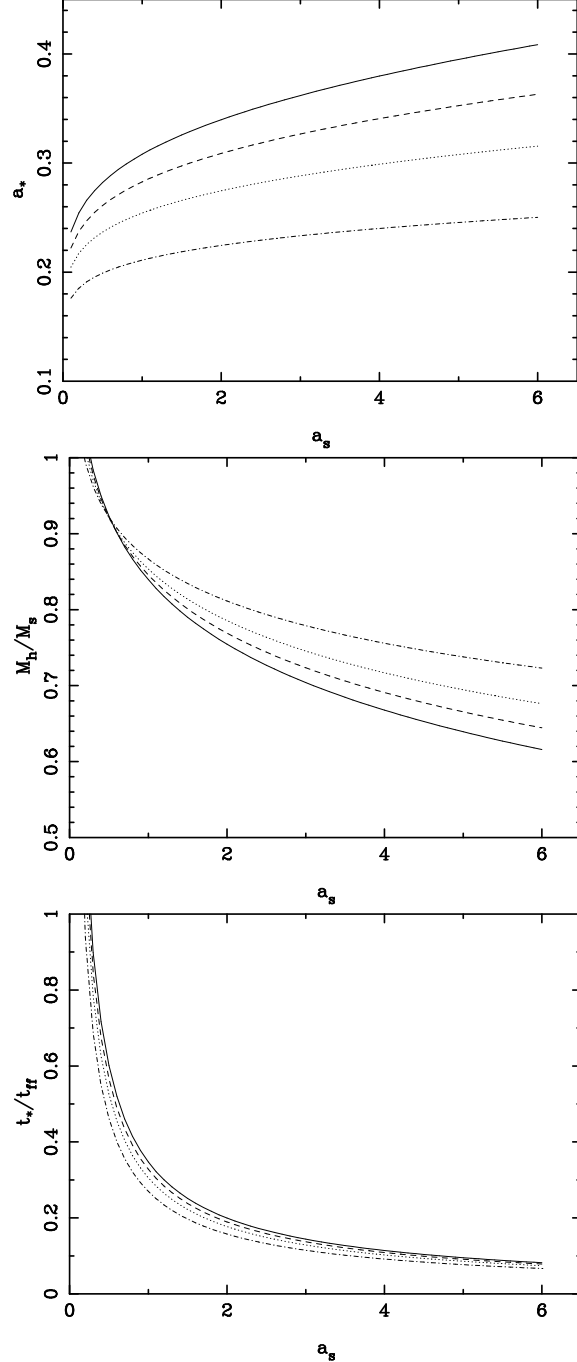


Figure 1. The black hole spin (top panel) and mass (middle panel) at the disk formation time as functions of the progenitor spin, a_s , for $M_c/M_s = 1/3$ (dash-dotted line), $1/5$ (dotted line), $1/9$ (dashed line), and $1/31$ (solid line). The bottom panel shows the time of disk formation as a function of a_s for the same models.

the outer regions of large disks will remain adiabatic. The accretion time of neutrino cooled disks

$$t_d \approx 2.6 \left(\frac{\alpha}{0.1}\right)^{-6/5} \left(\frac{r_d}{100}\right)^{4/5} \left(\frac{M_h}{10M_\odot}\right)^{6/5} \text{ s} \quad (14)$$

(Popham et al. 1999) is significantly less than the free-fall time scale

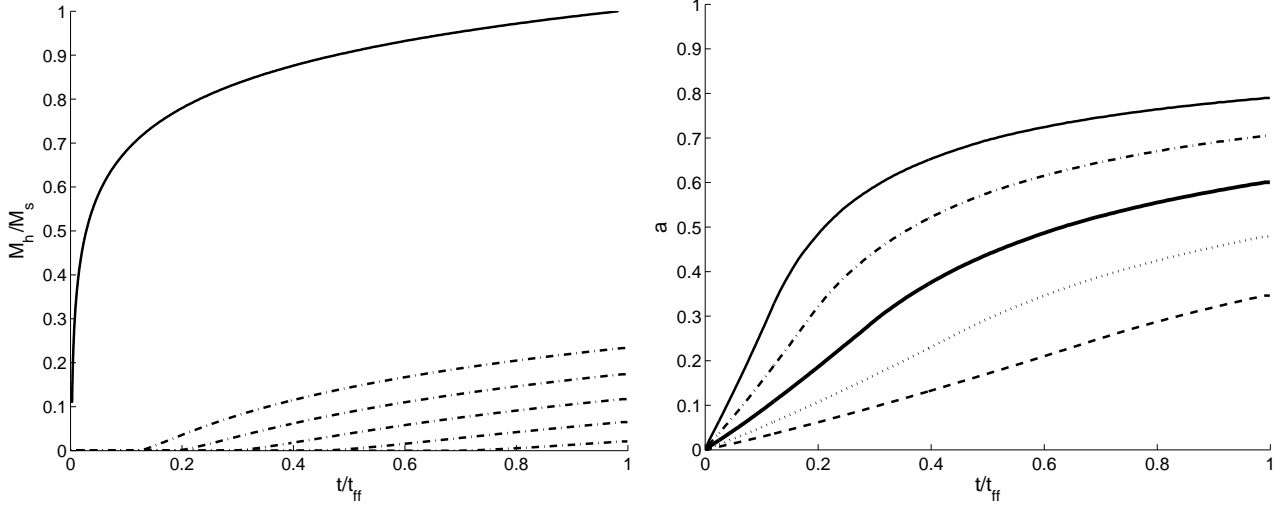


Figure 2. Evolution of the black hole mass and spin in the Bethe’s model with $M_c/M_s = 1/9$. *Left panel:* The total mass of black hole (solid line) and the mass accumulated via the accretion disk (dash-dotted lines) for the progenitor spin $a_s = 0.33, 0.58, 1.0, 1.7$, and 3 . The higher value of a_s correspond to the higher fraction of mass processed via the disk. *Right panel:* The spin parameter a of the black hole for the progenitor spin $a_s = 0.33$ (dashed line), 0.58 (dotted line), 1.0 (thick solid line), 1.7 (dot-dashed line), and 3.0 (thin solid line). The evolution time is given in the units of the free-fall time (see Eq.15).

$$t_{ff} \approx 240 \left(\frac{R}{R_\odot} \right)^{3/2} \left(\frac{M_s}{10M_\odot} \right)^{-1/2} \text{ s.} \quad (15)$$

The accretion time of large disks can be estimated using the α -model for slim disks ($\delta = H_d/R_d \simeq 0.3$)

$$t_d \approx 250 \left(\frac{\alpha\delta^2}{0.01} \right)^{-1} \left(\frac{r_d}{10^3} \right)^{3/2} \left(\frac{M_h}{10M_\odot} \right) \text{ s} \quad (16)$$

(Shakura & Sunyaev 1973). Thus, with the exception of largest disks, the time scale of disk accretion is shorter compared to the free-fall time scale, and hence the growth rate of the black hole mass is given directly by the rate of the collapse.

In order to estimate the mass and rotation rate of the black hole at the time of the disk formation one needs to know the mass distribution of progenitor at the onset of collapse. Here we adopt the power law model used by Bethe (1990) in his analytical models of core-collapse supernovae,

$$\rho(R) = \rho_c \left(\frac{R}{R_c} \right)^{-3}, \quad R > R_c, \quad (17)$$

where R_c is the radius of iron core. Simple integration allows us to find the following equations for the mass

$$M(R) = 4\pi\rho_c R_c^3 \ln(R/R_c) \quad (18)$$

and the moment of inertia

$$I(R) = \frac{1}{3} \frac{M(R)R^2}{\ln(R/R_c)} \quad (19)$$

of the shell between the iron core and the radius R .

By analogy with the black hole theory it is convenient to describe the rotation rate of collapsing star using the spin parameter

$$a_s = \frac{J_s c}{GM_s^2}. \quad (20)$$

In Bethe’s model it relates to Ω_s via

$$\Omega_s = a_s \frac{3GM_s(1+\eta)^2}{R_s^2 c} \ln y_s \quad (21)$$

where $y_s = R_s/R_c$, $\eta = M_c/M_s$, and we ignore the small contribution of compact iron core to the total spin of the star. The condition (2) with $q = 1$ implies that

$$a_s \leq \frac{1}{9 \ln y_s} r_s^{1/2} \simeq 5.2 \left(\frac{R}{R_\odot} \right)^{1/2} \left(\frac{M_s}{10M_\odot} \right)^{-1/2}, \quad (22)$$

where we used $y_s = 100$. This seems to suggest that the stellar collapse may lead to formation of rapidly rotating black holes.

Suppose that the disk is first formed at time t^* and that by this time the black hole has swallowed the star up to the initial radius $R = R_*$. Assuming that the black hole spin at this point is low, $a_* \ll 1$, we have

$$\Omega_s R_*^2 = (4 - a_*) \frac{G(M_* + \eta M_s)}{c}, \quad (23)$$

where $M_* = M(R_*)$. Using Eqs.(18) and (21) this condition can be written as the following algebraic equation for $y_* = R_*/R_c$

$$y_*^2 = \frac{(4 - a_*)y_s^2}{3(1 + \eta)^2 a_s \ln y_s} \left[\frac{\ln y_*}{\ln y_s} + \eta \right], \quad (24)$$

where

$$a_* = \frac{4}{1 + 3(\ln y_* + \eta \ln y_s)}. \quad (25)$$

This equation is solved numerically and the results are presented in Fig.1. One can see that the disk is formed relatively late, with the typical time $t_* > 0.1t_{ff}$, when more than a half of the star has already collapsed into the black hole. However, the black hole spin at this moment is relatively low, $0.2 < a_* < 0.4$.

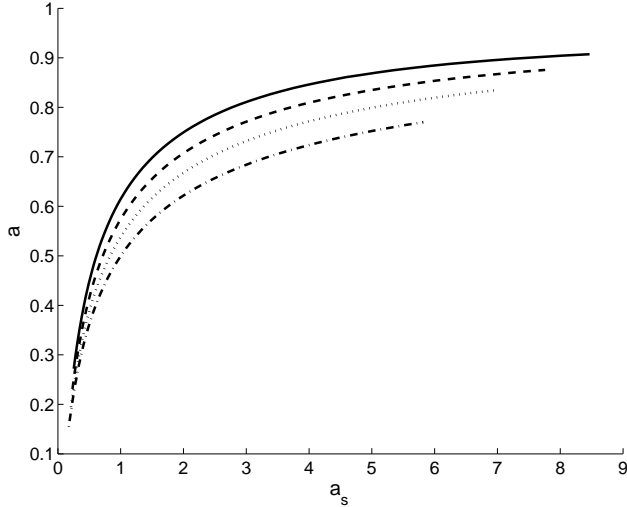


Figure 3. The final value of the black hole spin in Bethe’s model with a as a function of the progenitor spin for models with $M_c/M_{star} = 1/3$ (dot-dashed line), $1/5$ (dotted line), $1/9$ (dashed line), and $1/31$ (solid line).

3 GROWTH OF BLACK HOLES

In order to explore the evolution of the black hole spin for more sophisticated models of LGRB progenitors, as well as its evolution in Bethe’s model after the disk formation, one can integrate the following system of dynamic equations

$$\frac{dM_h}{dR} = 4\pi R^2 \rho(R), \quad (26)$$

$$\frac{dJ_h}{dR} = 4\pi R^2 \rho(R) \int_0^{\pi/2} \tilde{l}(R, \theta) \sin \theta d\theta. \quad (27)$$

Here, $\rho(R)$ is the stellar mass density prior to the collapse and $\tilde{l}(R, \theta)$ is the specific angular momentum retained by the fluid element, initially located at the point with the coordinates $\{R, \theta\}$, by the time it crosses the event horizon. This quantity is given by

$$\tilde{l} = \begin{cases} l(R, \theta) & \text{if } l < l_{mb}(M_h, J_h) \\ l_{ms}(M_h, J_h) & \text{if } l > l_{mb}(M_h, J_h) \end{cases}, \quad (28)$$

where $l(R, \theta)$ is the distribution of the progenitor’s angular momentum. The initial conditions for Eqs.(26,27) correspond to the iron core of the WR star

$$M_h(R_c) = M_c, \quad J_h(R_c) = 0, \quad (29)$$

where M_c and R_c are respectively the mass and the radius of the core. When the accretion rate is determined by the free-fall time, R and t can be related via

$$t^2 = \frac{2R^3}{9GM(R)}. \quad (30)$$

The same approach has been used in Janiuk et al. (2008) in their search for the laws of rotation that would fit the collapsar model of LGRBs. They did not consider

the solid body rotation⁵ and assumed that initially the black hole is rapidly rotating, with $a = 0.85$. They also used the model of geometrically thick and radiatively inefficient disk, with the inner edge located at the radius of the marginally bound orbit, whereas we use the thin disk approximation, which is more suitable for the neutrino-cooled collapsar disks.

3.1 Bethe’s model

Figure 2 shows the typical evolution of the black hole mass and spin, as described by Eqs.26 and 27, for the Bethe’s model. One can see that the black hole spin increases significantly above the values attained by the time of disk formation. Eventually, it reaches the relatively high values of $a = 0.3 - 0.8$, the final spin depending mainly on the progenitor spin and less so on the mass fraction of the iron core (see Fig.3). These higher values of a imply higher potential efficiency of both the neutrino annihilation and the Blandford-Znajek mechanisms of the LGRB jet production (Popham et al. 1999; Zalamea & Beloborodov 2009; Barkov & Komissarov 2008a).

The total mass accretion rate can be easily derived from the mass distribution and the free fall time (see Eq.30):

$$\dot{M} = \frac{2}{3} \frac{M_s}{\ln y_s} t^{-1} \simeq 1.45 \left(\frac{M_s}{10M_\odot} \right) \left(\frac{t}{1s} \right)^{-1} M_\odot s^{-1}, \quad (31)$$

where t is the time since the start of the collapse. As one can see in Figure 2, soon after the disk formation the mass accretion rate becomes dominated by disk. Initially, the rate can be rather high but at around $t \simeq 100s$ it becomes insufficient for the neutrino annihilation mechanism to operate.

3.2 Stellar evolution models

Although the Bethe’s model provides a reasonable zero-order approximation for the structure of pre-supernova stars, the more sophisticated models based on numerical integration of the equations of stellar evolution yield somewhat different stellar structure with wealth of finer details. Our next results are based on the pre-collapse structure of massive zero age main sequence (ZAMS) stars with masses $M_s = 20M_\odot$ and $35M_\odot$ described in Heger et al. (2004). Assuming that stars of close binaries lose their extended envelopes we cut of the mass distributions beyond the C/O core. This results in the progenitors with masses $M_s = 6.15M_\odot$ (model A) and $M_s = 12.88M_\odot$ (model B) respectively, and radius $R_s \simeq 0.3R_\odot$.⁶ The moments of inertia of models A and B are $I \simeq 0.065M_s R_s^2$ and $0.074M_s R_s^2$ respectively. Given these parameters, Eqs.1 and 2 imply the

⁵ The solid body rotation law was studied in Janiuk & Proga (2008) but it was assumed there that the black hole was non-rotating.

⁶ This radius is rather small, twice as small compared to the models of WR stars constructed in Schaerer & Maeder (1992) and 10-20 time smaller compared to the observed radii (Cherepashchuk & Mofat 1994; Crowther 2007). We can offer no clear explanation for this discrepancy. Perhaps, the artificial “removing” of extended H/He envelope is not a particularly accurate procedure.

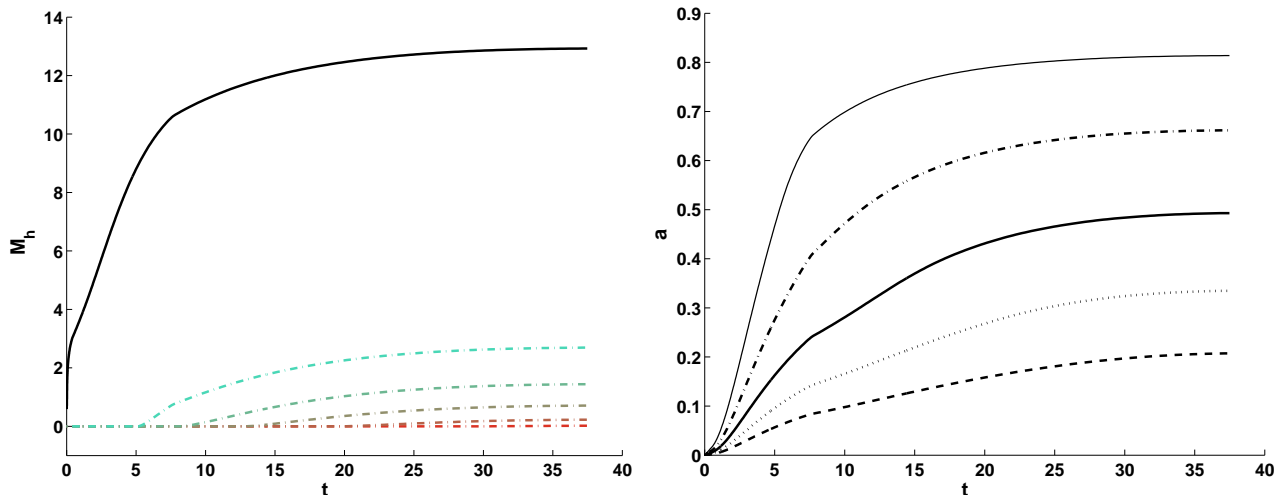


Figure 4. Evolution of black hole’s mass and spin in numerical model B. *Left panel:* The total mass of black hole (solid line) and the mass accumulated via the accretion disk (dash-dotted lines) for the progenitor spin $a_s = 0.20, 0.33, 0.57, 0.96$, and 1.6 . The higher value of a_s correspond to the higher fraction of mass processed via the disk. *Right panel:* The spin parameter a of the black hole for the progenitor spin $a_s = 0.20$ (dashed line), 0.33 (dotted line), 0.57 (thick solid line), 0.96 (dot-dashed line), and 1.6 (thin solid line)

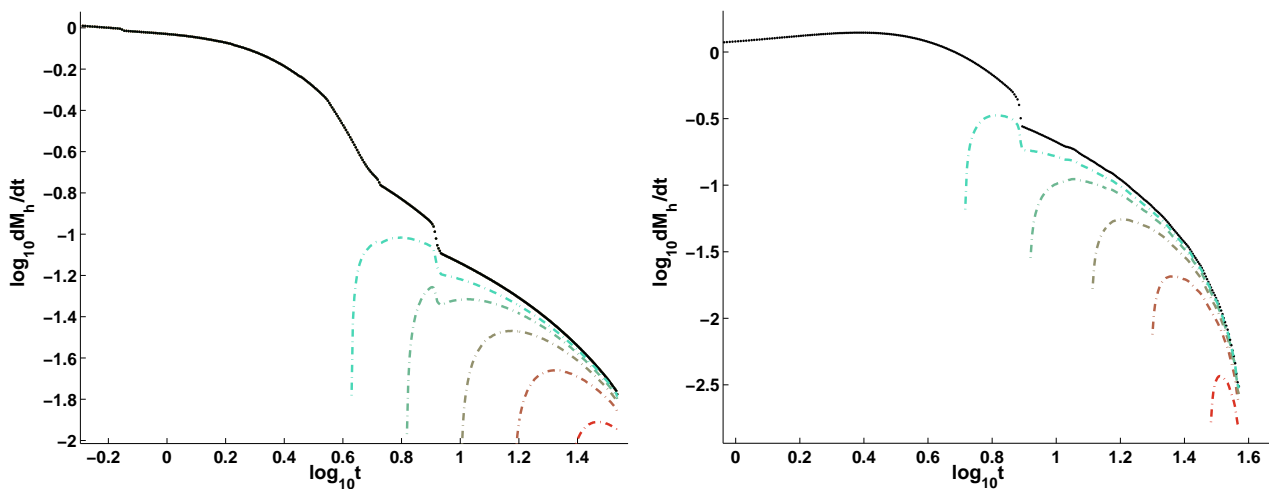


Figure 5. The accretion rate (in the units of $M_\odot \text{ s}^{-1}$) for model A (left panel) and model B (right panel). The solid lines show the total accretion rate whereas the dash-dotted lines show the disk accretion rates for different spins of the progenitor; $a_s = 0.32, 0.54, 0.90, 1.52$, and 2.55 for model A and $a_s = 0.20, 0.33, 0.57, 0.96$, and 1.6 for model B. Higher values of a_s correspond to earlier formation of accretion disk and higher disk accretion rates.

spin parameters $a_s < 2.6$ and $a_s < 1.7$ for the models A and B respectively; somewhat smaller than in the Bethe’s model.

Figure 4 shows the evolution of the black hole’s mass and spin in model B for different assumed values of the progenitor’s spin. The comparison with the results obtained for Bethe’s model shows only relatively minor differences, suggesting that Bethe’s model is quite accurate. Figure 5 shows the accretions rates, both for the disk and in total, for different progenitor spins in models A and B. One can see that initially the disk accretion rate grows rapidly and soon it accounts for most of the total accretion rate. Then it begins to decay, approximately as t^{-1} in model A and t^{-3} in Model B. For the cases with faster stellar rotation, the peak disk

accretion rate is sufficiently high to ensure effective neutrino cooling of the disk (Chen & Beloborodov 2007).

3.3 Polytrope model

Finally, we consider the model polytrope with index $n = 3$, which could be used to describe the cores of most massive stars at the pre-supernova phase (Tutukov & Fedorova 2007). In this model the concentration of mass towards the centre is much weaker, resulting in higher moment of inertia and larger angular momentum compared to the Bethe’s model with the same mass, radius and rotation frequency. Even if we consider models with the same spin parameter a_s , the polytrope yields generally higher fraction of mass accreted via the accretion disk and more rapidly rotating

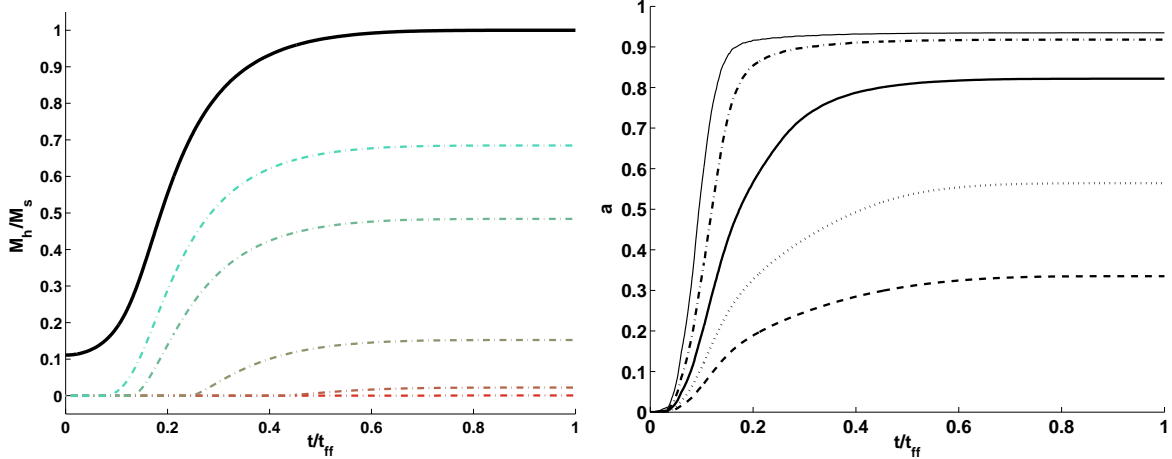


Figure 6. The evolution of black hole’s mass and spin in the polytrope model of progenitor with the initial black hole mass $M_c = M_s/9$. The left panel shows the total mass of the black hole (thick solid line) as well as the mass accumulated via the accretion disk for different rotation rates of the progenitor, $a_s = J_s c/GM_s^2 = 0.33, 0.58, 1.0, 1.7, 3.0$ (dash-dotted lines). Faster rising lines correspond to higher rotation rate. The right panel shows the spin parameter of the black hole, a , for the same values of a_s .

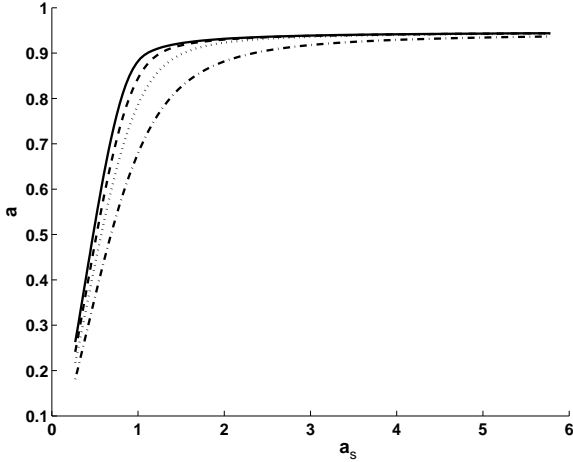


Figure 7. The evolution of black hole spin for polytropic models with $a_s = 3$ and $M_c/M_s = 1/3$ (dot-dashed line), $1/5$ (dotted line), $1/9$ (dashed line), and $1/31$ (solid line).

black holes (see Figure 6). Similarly to other models, the final value of the black hole’s spin does not show strong dependence on the iron core mass fraction, at least for $M_c/M_s \in (1/3, 1/31)$ (see Figure 7).

The polytrope model was also used to test our calculations against the fully general relativistic simulations by Shibata & Shapiro (2002). For the polytropic star with angular momentum $a_s = 1$ our model gives a black hole with $M_b = 0.90M_s$ and $a = 0.76$ by the time of disk formation. This is in excellent agreement with the numerical simulations which give $M_b = 0.90$ and $a = 0.75$.

4 JET SIMULATIONS

The analysis carried out in Sections 2 and 3 suggests that during the collapse of a WR star in a very close binary system, the conditions can become favourable to production of

LGRB jets either via the neutrino heating or the Blandford-Znajek mechanism. Although the production of jets via the Blandford-Znajek mechanism has already been studied numerically in several previous papers the conditions suggested by the binary scenario are different from those explored so far. By the time of the accretion disk formation the black hole is much more massive compared to the usually assumed $M_h \simeq 2M_\odot$. Its rotation rate is noticeably lower compared to $a \simeq 1$, assumed in the past. Finally, the progenitor’s rotation is not differential but uniform. These differences invite additional numerical simulations to explore the new region of parameter space.

4.1 Setup of Simulations

The progenitor model describes a compact WR star of radius $R_s = 3 \times 10^{10}$ cm and rotation period $T_s = 1.4$ hr; the corresponding specific angular momentum on the stellar equator is $l_s = 1.13 \times 10^{18}$ cm²s⁻¹. The progenitor’s magnetic field is assumed to be purely poloidal and uniform, with the strength $B_0 = 1.4 - 8.4 \times 10^7$ G.

Simulations of this type are computationally expensive even in 2D. On the other hand, the early stages of the collapse are very simple and can be treated analytically with sufficient accuracy. For these reasons, we start simulations only after the expected time of the disk formation, $t_s = 17$ s. Based on the analysis given in the previous sections, the black hole mass is set to $M_h = 10M_\odot$ and the mass accretion rate to $0.14M_\odot$ s⁻¹. The initial radial distributions of mass and velocity are the same as in the Bethe model:

$$\rho \propto R^{-3/2}, \quad v^r = (2GM_h/R)^{1/2}. \quad (32)$$

The initial distributions of angular momentum and magnetic field are derived from the progenitor distributions by taking into account the distortions caused by the free-fall collapse over the time t_s :

$$l(R, \theta) = \Omega_s (R \sin \theta)^2 \left(1 + \frac{t_s}{t_{ff}(R)} \right)^{4/3}, \quad (33)$$

Table 1. Numerical models.

Model	a	B_0	Ψ_{28}	L_{BZ}	\dot{M}_h	$L_{BZ}/\dot{M}_h c^2$
M1	0.6	1.4	0.46	—	—	—
M2	0.6	4.2	1.5	0.44	0.017	0.0144
M3	0.45	8.4	3.1	1.1	0.012	0.049

a is the black hole spin; B_0 is the initial magnetic field strength in the units of 10^7G ; Ψ_{28} is the magnetic flux accumulated by the black hole by the time of explosion in the units of 10^{28}G cm^2 ; L_{BZ} is the total power of the BZ-mechanism during the explosion in the units of 10^{51}erg/s ; \dot{M}_h is the black hole mass accretion rate during the explosion in the units of $M_\odot \text{s}^{-1}$.

$$B^r = \frac{B_0 \sin \theta \cos \theta}{\sqrt{\gamma}} R^2 (1 + t/t_{ff}(R))^{4/3}, \quad (34)$$

$$B^\theta = \frac{B_0 \sin^2 \theta}{2\sqrt{\gamma}} 2R (1 + t/t_{ff}(R))^{1/3}, \quad (35)$$

where $t_{ff}(R) = \sqrt{2R^3/9GM_h}$ is the local free fall time scale and γ is the determinant of the metric tensor of space (see Appendix A). In these simulations we studied three different cases summarised in Table 1.

The simulations were carried out with 2D axisymmetric GRMHD code described in Komissarov (1999, 2004). The gravity effects are introduced via the Kerr metric with fixed parameters; the Kerr-Schild coordinates are used in order to avoid the coordinate singularity at the horizon. The computational grid is uniform in the polar angle, θ , where it has 180 cells and logarithmic in the spherical radius, R , where it has 445 cells. The inner boundary is located just inside the event horizon and adopts the free-flow boundary conditions. The outer boundary is located at $R = 8.3 \times 10^9 \text{cm}$ and at this boundary the flow is prescribed according to the Bethe's model.

In the simulations we used realistic equation of state (EOS) that takes into account the contributions from radiation, lepton gas (including pair plasma), and non-degenerate nuclei (hydrogen, helium, and oxygen). This is achieved via incorporation of the EOS code HELM (Timmes & Swesty 2000), The neutrino cooling is computed assuming optically thin regime and takes into account URCA-processes (Ivanova et al. 1969), pair annihilation, photo-production, and plasma emission (Schinder et al. 1987), as well as synchrotron neutrino emission (Bezchastnov et al. 1997). In fact, URCA-processes strongly dominate over other mechanisms in this problem. Photo-disintegration of nuclei is included via modification of the EOS following the prescription given in Ardeljan et al. (2005). The equation for mass fraction of free nucleons is adopted from Woosley & Baron (1992). We have not included the radiative heating due to annihilation of neutrinos and antineutrinos produced in the accretion disk mainly because this requires elaborate and time consuming calculations of neutrino transport.

4.2 Results

In general, the results of these simulations are in agreement with our previous studies (Barkov & Komissarov 2008a,b; Komissarov & Barkov 2009). Because of the modified setup, which corresponds to the later stages of the collapse, the accretion disk is formed straight away. At the same

time, the accretion shock separates from the disk surface and quickly expands up to $R \simeq 100 - 200 R_g$. In the model M1, the shock then begins to oscillate and no jets emerge by the end of the simulations, $t = 19.5 \text{s}$. In contrast, both the models M2 and M3 eventually develop polar jets of relativistic plasma which are powered via the Blandford-Znajek mechanism (see Figs.8 and 9). These results comply with the BZ activation condition, $\kappa \geq 0.2$, where

$$\kappa = \frac{\Psi}{4\pi r_g \sqrt{\dot{M} c}}, \quad (36)$$

is the activation parameter, Ψ is the magnetic flux threading the black hole and \dot{M} is the mass accretion rate of the collapsing star (Komissarov & Barkov 2009). For the parameters of the present simulations we have $\kappa \simeq 0.07 \Psi_{28}$, where the magnetic flux is given in the units of 10^{28}G cm^2 , and, thus, one would expect the BZ mechanism to become activated for $\Psi_{28} > 3$. As one can see from the data presented in Table 1 which was indeed the case.

According to the simple monopole model of black hole magnetosphere, the power of the BZ mechanism is

$$\dot{E}_{BZ} = 1.4 \times 10^{51} f_2(a) \Psi_{28}^2 \left(\frac{M_b}{10 M_\odot} \right)^{-2} \text{erg s}^{-1}, \quad (37)$$

where $f_2(a) = a^2 (1 + \sqrt{1 - a^2})^{-2}$ (Barkov & Komissarov 2008a). Like in our previous simulations, the direct measurements of energy flux across the BH horizon roughly agree with this result (see Table 1).

One significant difference with the results of previous simulations is the development of a one-sided jet in model M2. Although noticeable deviations from the equatorial symmetry have been observed before, in particular the asymmetric oscillations of the accretion shock, such a strong deviation is observed for the first time. The initial solution is not exactly symmetric because of the rounding errors, but they are tiny and the observed braking of the equatorial symmetry has to be rooted in the nonlinear dynamics of the flow. It appears that the accretion flow, which is deflected towards the equatorial plane at the oblique shock driven by the northern jet, protrudes into the southern hemisphere. There it collides with the accretion flow of the southern hemisphere and together they stream towards the black hole's southern pole, thus suppressing the development of a southern jet.

If persistent, such a one-side jet could impart a strong kick on the black hole and the binary, significantly altering its motion in the parent galaxy (Fragos et al. 2009). The maximum kick velocity can be estimated as

$$v_{kick} = \frac{E_{jet}}{c M_h} \approx 170 \left(\frac{E_{jet}}{10^{52} \text{erg}} \right) \left(\frac{10 M_\odot}{M_h} \right) \text{km s}^{-1}, \quad (38)$$

which is consistent with the observations of the X-ray binary XTEJ1118+480 (Gualandris et al. 2005). However, at present we cannot say whether such one-sidedness can persist during the life-time of LGRB or this is just a transient phenomenon.

5 MERGER SCENARIO

The case of close tidally-locked binary considered above involves binaries with orbital separation very close to the size

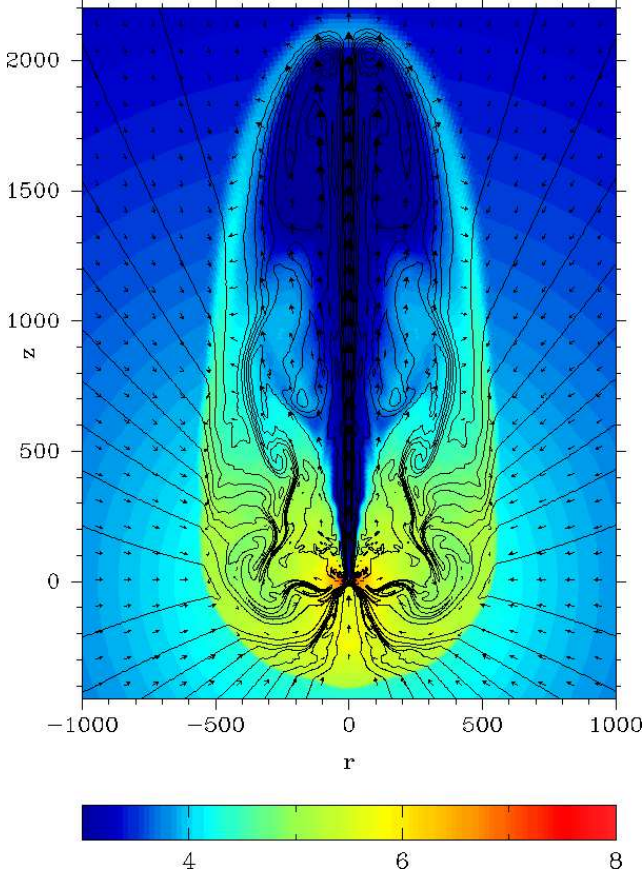


Figure 8. Model M2 ($B_0 = 2.2 \times 10^7 \text{G}$, $a = 0.6$) at the time of $t = 1.35\text{s}$ after the start of simulations (18.3s after the start of the stellar collapse). The colour image shows the baryonic rest mass density, $\log_{10}\rho$, in CGS units, the contours show the magnetic field lines, and the arrows show the velocity field.

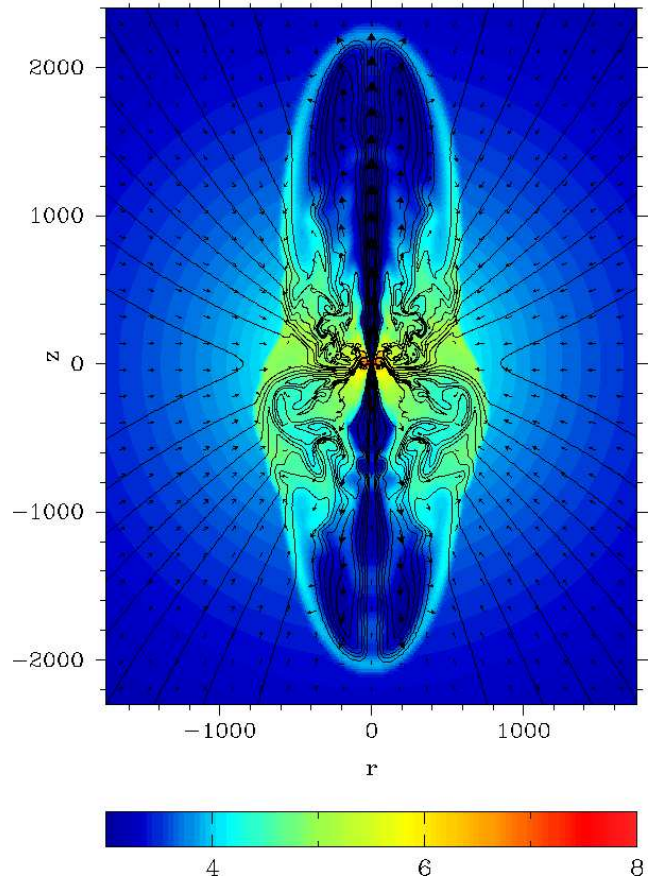


Figure 9. Model M3 ($B_0 = 8.8 \times 10^7 \text{G}$, $a = 0.45$) at $t = 1.35\text{s}$ after the start of simulations (18.3s after the start of the collapse). The colour image shows the baryonic rest mass density, $\log_{10}\rho$, in CGS units, the contours show the magnetic field lines, and the arrows show the velocity field.

of the Roche lobe of the WR star and this suggests to go one step further and consider the case of even smaller separation which can lead to the common envelope evolution resulting in a merger of the binary (Tutukov & Yungelson 1979) and GRB explosion (Zhang & Fryer 2001). Such a merger can be divided into three phases. During the first phase, the compact companion spirals inside the extended envelope of the normal star and spins it up via deposition of its orbital angular momentum. The compact star also increases its mass and spin via the Bondi-type accretion. According to the simulations of Zhang & Fryer (2001), during the last 500s of the in-spiral the compact star can accumulate up to $3.5M_\odot$. Thus, the mean accretion rate is less than $10^{-2}M_\odot/\text{s}$ implying inefficient neutrino heating.

The second stage begins when the compact star approaches the centre of its WR companion and the accretion rate increases. Zhang & Fryer (2001) find that in the case of $16M_\odot$ companion the neutrino annihilation mechanism can operate for around 60 seconds and release about 10^{52}erg . This is more than enough to drive a supernova explosion. For the companion mass below $8M_\odot$ the neutrino heating is too weak and the second phase is absent.

The third phase takes place if the second phase does not result in the supernova explosion or if the explosion is highly non-spherical and does not remove the equatorial lay-

ers of the WR star. During this phase the compact object, already a black hole, accretes these layers, which have been spun up during the first phase. Assuming that the mass of the compact star is small compared to the mass of its WR companion, its orbital angular momentum can be found via the Keplerian law

$$J_c(R) = M_c \sqrt{GM(R)R},$$

where $M(R)$ is the WR mass inside the radius R . As the compact star moves from the radius R to $R + dR$, it transfers the angular momentum $dJ_c(R) = (dJ_c/dR)dR$ to the envelope of the WR star. Assuming that most of this angular momentum is transferred to the mass $dM = (dM/dR)dR$ of the envelope located between R and $R + dR$, we obtain the specific angular momentum of the envelope after the merger as

$$l \simeq \frac{dJ_c}{dM} = \frac{dJ_c/dR}{dM/dR}.$$

For the Bethe's model, where $M(R)$ is given by Eq.(18), this gives

$$l \simeq \frac{M_c}{2} \left(\frac{GR}{M(R)} \right)^{1/2} (1 + \ln(R/R_c)), \quad (39)$$

which is smaller than the local Keplerian angular momentum

provided $M(R) > M_c(1 + \ln R/R_c)/2$. This suggests that if $M_s \gg M_c$ then only a small fraction of the common envelop is lost during the merger. For $R = R_s$ this equation gives

$$l \simeq 5.2 \times 10^{18} \left(\frac{M_c}{2M_\odot} \right) \left(\frac{R_s}{R_\odot} \right)^{1/2} \left(\frac{M_s}{10M_\odot} \right)^{-1/2} \text{ cm}^2 \text{ s}^{-1}. \quad (40)$$

In the α -model, the accretion time scale of the disk with such angular momentum can be estimated via

$$t_d \simeq \frac{1}{\alpha \delta^2} \frac{l^3}{(GM_s)^2} = \simeq 8000 \text{ s} \left(\frac{\alpha \delta^2}{0.01} \right)^{-1} \left(\frac{R_s}{R_\odot} \right)^{3/2} \left(\frac{M_c}{2M_\odot} \right)^2 \left(\frac{M_s}{10M_\odot} \right)^{-7/2}. \quad (41)$$

This is significantly longer than the duration of the stellar collapse (see Eq.15). In fact, such a long time scale suggests the possibility of explaining the phase of shallow decay and late flares in the X-ray light curves of LGRBs discovered by *Swift* (Zhang 2007; Chincarini et al. 2007).

To find the mass accretion rate as a function of time we note that

$$\dot{M} = \frac{dM}{dt_d} = \frac{dM/dR}{dt_d/dR}.$$

Using Eqs.(18,41,39) to evaluate dM/dR and dt_d/dR we obtain⁷

$$\dot{M} \simeq \frac{2}{3} \frac{M_s}{\ln(R_s/R_c)} \frac{1}{t} \simeq 1.45 \left(\frac{M_s}{10M_\odot} \right) \left(\frac{t}{1\text{s}} \right)^{-1} \frac{M_\odot}{\text{s}}. \quad (42)$$

Thus, on the time scale of $10^3 - 10^4$ s the mass accretion rate is very low, $\dot{M} \simeq 10^{-3} \div 10^{-4} M_\odot \text{ s}^{-1}$, ruling out the neutrino mechanism and leaving the BZ mechanism clear favourite. Indeed, the maximum possible amount of magnetic flux that can be accumulated by the black hole is given by the balance of magnetic pressure and the gas pressure of the accretion disk,

$$\frac{B_{max}^2}{8\pi} \simeq P_g \simeq \rho c_a^2, \quad (43)$$

where c_a is the sound speed. If we utilize the model of α -disk and estimate the magnetic field strength at the gravitational radius then the corresponding magnetic flux will be

$$\Psi_{max} \simeq 3 \times 10^{29} \left(\frac{\alpha \delta}{0.03} \right)^{-1/2} \left(\frac{M_b}{10M_\odot} \right) \dot{M}_1^{1/2} \text{ G cm}^2, \quad (44)$$

where \dot{M}_1 is the mass accretion rate in the units of M_\odot/s . Even for \dot{M}_1 as small as 10^{-4} this equation gives the substantial value of $\Psi_{max} \simeq 3 \times 10^{27} \text{ G cm}^2$. The corresponding BZ power, $\dot{E}_{BZ} \simeq 2.2 \times 10^{49} \text{ erg/s}$, is more than sufficient to explain the X-ray observations, allowing the magnetic field to be even weaker compared to the value suggested by Eq.43.

6 DISCUSSION AND CONCLUSIONS

One of the main issues of this study was to investigate the efficiency of the tidal spin up in close massive binaries in the context of the collapsar model of LGRBs. In particular, we

wanted to find out the typical masses and spins of the black holes formed during the collapse of WR companion. It turns out, that the BH spin in this model is rather modest. For example, in the most optimistic case of a binary with the smallest possible orbital separation, the spin parameter of the WR star is relatively high, $a_s \simeq 6$, and one may have expected the BH to be rapidly rotating. However, we find that the spin parameter is only $a \simeq 0.4$ at the time of the accretion disk formation, and $a \simeq 0.8$ by the end of the stellar collapse, which is significantly lower than the maximally possible value $a = 1$. This is mainly due to the significant loss of angular momentum suffered by the mass accreted via the disc; the rejected angular momentum is either stored in the remote part of the accretion disk or removed by a disk wind. Indeed, as soon as the accretion disc is formed, the rate of accretion of angular momentum slows down significantly. Moreover, by the time of the disk formation the black hole mass is already rather high, exceeding half of the progenitor mass prior to the collapse. Thus, the black hole simply runs out of accreting matter before its rotation can approach the maximal possible rate (cf. Thorne 1974).

The mass accretion rate in this scenario is much lower compared to the usual $\dot{M} = (0.1 \div 1) M_\odot \text{ s}^{-1}$ invoked in the standard collapsar model (MacFadyen & Woosley 1999). This makes the neutrino mechanism less attractive compared to the magnetic mechanisms, and the BZ-mechanism in particular. In fact, the very rapid decline in the efficiency of neutrino mechanism below $\dot{M} \leq 0.02 - 0.05 M_\odot \text{ s}^{-1}$ (Popham et al. 1999; Zalamea & Beloborodov 2009) makes the explanation of the LGRB bursts with duration ≥ 100 s rather problematic even within the standard collapsar model due to the low mass accretion rate expected on such time scale (see Eq.42 and Fig.5).

However, the BZ mechanism could have its own difficulties in this scenario. Indeed, it requires very strong ordered magnetic field. For example, in order to provide the power of $10^{50} \text{ erg s}^{-1}$ the black hole of mass $10 M_\odot$ and $a = 0.6$ should accumulate the magnetic flux of order $\Psi = 8 \times 10^{27} \text{ G cm}^2$. The magnetic flux necessarily to activate the BZ mechanism soon after the formation of accretion disk is even higher. According to Table I this is of the order $\text{few} \times 10^{28} \text{ G cm}^2$. Perhaps the free-fall accretion rate set up in our simulation is a bit too high and could have been reduced by a factor of 10. However according to Eq.(36), this would reduce the critical value of magnetic flux only by a factor of 3.

The origin of such strong field is not clear. It could be generated via magnetic dynamo in the accretion disc (e.g. Brandenburg et al. 1995) or in the convective core of the progenitor (e.g. Charbonneau & MacGregor 2001). It may also be inherited by the progenitor from the interstellar medium (ISM) during its formation (e.g. Braithwaite & Spruit 2004). The current status of both the stellar and disk dynamo theories does not really allow to make reliable conclusions. Even the issue of advection of externally generated magnetic field by the accretion disk onto the central black hole is still unresolved (e.g. Bisnovatyi-Kogan & Ruzmaikin 1974; van Ballegoijen 1989; Guan & Gammie 2009; Spruit & Uzdensky 2005; Rothstein & Lovelace 2008; Igumenshchev 2008). There seems to be a general agreement that accretion disks produce mainly azimuthal magnetic field and unable to generate poloidal field on scales exceeding the disk height. The

⁷ This equation is the same as Eq.31 but t spans a different range of timescales, now dictated by the disc accretion time.

magnetic dynamo in convective cores of massive stars could be more promising in this respect. For example, from the results of Charbonneau & MacGregor (2001) it seems possible to generate up to $\Phi \simeq 10^{28} \text{ G cm}^2$ in the convective cores of B stars.

By design, our numerical simulations cannot address the issue of magnetic field generation in accretion disks and strictly-speaking deal only with the fossil model of magnetic field. The numerical results by Braithwaite & Spruit (2004) suggest that strong fossil field can relax to a simple ordered configuration with dipolar poloidal field on a relatively short time scale, which makes our setup not that unrealistic. However, further studies are required to verify this model. The observations of massive stars do not support magnetic flux of order 10^{28} G cm^2 and higher. The current record is held by θ^1 Ori C, whose dipolar magnetic flux $\Psi \simeq 2 \times 10^{27} \text{ G cm}^2$, Donati et al. (2002)). One may speculate that most of the magnetic flux is hidden in the stellar interior. Indeed, the resistive time scale across the extended radiative outer layers of massive stars exceeds their life time by many orders of magnitude Braithwaite & Spruit (2004).

The fact that the magnetic flux of neutron stars is less than 10^{27} G cm^2 also seems to be working against the fossil hypothesis. However, neutron stars are collapsed compact Fe cores of massive stars. The typical cross section of such a core is several orders of magnitude below that of the whole star and, thus, the core may account only for a small fraction of the total magnetic flux hidden inside the supernova progenitor.

The host galaxies of LGRBs show strong evidence of enhanced star formation (Bloom et al. 1998; Sokolov et al. 2001; Fruchter et al. 2006). It is interesting that the recent observations of such starburst galaxies also indicate strong ISM magnetic field, in fact up to ten times stronger compared to the Milky Way (Beck & Krause 2005; Beck 2008). This suggests that magnetization of young stars in the host galaxies of LGRBs can be abnormally high as well.

Another interesting proposal stems from the theory of Sun's magnetic activity proposed by Uzdensky (2007). In particular, he argued that fast reconnection can only operate in collisionless plasma and in the collisional regime the reconnection rate reduces to the much slower rate of Sweet-Parker. Since the collapsar plasma is collisional even in the rarefied funnel of the accretion disk then, according to this theory, the reconnection rate in the black hole magnetosphere can be relatively slow. An additional unexplored factor in the LGRB context is the effects of quantum physics on magnetic reconnection. Indeed, the expected magnetic field strength is well above the quantum value of $B_q = m_e^2 c^3 / \hbar e = 4 \times 10^{13} \text{ G}$. One may speculate that under this conditions the reconnection rate becomes even slower.

In the case of slow reconnection, the black hole may be able to build strong magnetic field via collecting the alternating magnetic field generated in the accretion disk. Since the magnetic stresses are invariant with respect to change of magnetic polarity such striped structure of magnetic field has no effect on the efficiency of the BZ-mechanism. Further downstream of the LGRB flow, where its plasma becomes collisionless or the magnetic field becomes sufficiently weak, the reconnection accelerates. However, as long as this occurs beyond the Alfvén surface, which for a black hole with reasonable spin does not greatly exceed the gravi-

tational radius, this does not disrupt the near magnetosphere of the black hole and does not reduce the efficiency of the BZ-mechanism. Moreover, such delayed reconnection could promote bulk acceleration of the LGRB flow (Drenkhahn & Spruit 2002).

Finally, the neutrino heating of the polar region, not included in our analysis and simulations, may also play a very important role, by initiating the LGRB outflow and creating the low density channel in the polar direction early on, when the mass accretion rate is still sufficiently high for effective neutrino-antineutrino annihilation. This would allow the BZ-mechanism to be activated along the field lines filling the channel even if the black hole magnetic flux is much lower compared to the values quoted above. Later on, when the mass accretion rate drops and the neutrino mechanism can no longer provide sufficient power, the BZ-mechanism can take over the role of main driver of the LGRB flow. One may even contemplate the scenario where the GRB precursors are related to the neutrino-driven stellar explosions and the main bursts to the magnetically-driven BH jets unleashed in the space cleared up by the blast. The delay between the two phases could be related to the disruption of the accretion flow by the supernova blast (Wang & Meszaros 2007). Because of the rotational effects the disruption may not be as severe in the equatorial direction, compared to the polar direction, as in the one-dimensional simulations by MacFadyen et al. (2001), leading to shorter fallback time-scales. The magnetic jets, though very powerful, could be less disruptive compared to the neutrino-driven jets because the magnetic hoop stress, associated with the azimuthal component of magnetic field, makes the sideways expansion of the jet cocoon less effective.

The most interesting, in view of the recent *Swift* observations of LGRB afterglows, version of the close binary scenario for GRB progenitors is the common envelope case, where the compact star, either a black hole from the onset or a neutron star which eventually collapses into a black hole, spirals inside the normal WR star. The large angular momentum transferred to the external layers of the WR star quite naturally leads to long accretion time scales, $\simeq 10^4 \text{ s}$. Thus, the central engine of LGRB jets arising in this scenario could operate for a sufficiently long time to explain the shallow phase of the X-ray light curves discovered by *Swift* (Zhang 2007). The X-ray flares, which are often seen during this phase, may result from the gravitational instabilities developing in this disc (Perna et al. 2006). Although the BZ mechanism is not that sensitive to the mass accretion rate as the neutrino mechanism, some dependence is still expected. For example, Eqs.(37,44) suggest that the power of the BZ mechanism may be proportional to the mass accretion rate. This can explain why the gamma ray emission becomes undetectable on the time-scale of the shallow decay of X-ray afterglows.

The extremely high rotation rates, about 50% of the break-up speed, assumed in the single progenitor model by Yoon & Langer (2005) and Woosley & Heger (2006) imply that in this model the outer layers of the collapsing star can also develop long-lived accretion disk. Indeed, in the “showcase” model 16TI of Woosley & Heger (2006) the outer $\simeq 2M_\odot$ have the specific angular momentum increasing outwards from 10^{18} to $10^{19} \text{ cm}^2 \text{ s}^{-1}$ at the pre-supernova phase. According to Eq.40 this corresponds to the disc ac-

cretion time scales of order 10^4 s. However, such a long time scale still rules out the neutrino annihilation as the mechanism for powering the collapsar jets.

ACKNOWLEDGMENTS

This research was funded by STFC under the rolling grant “Theoretical Astrophysics in Leeds” (SSK and MVB). The numerical simulations were carried out on the St Andrews UK MHD cluster and on the Everest cluster of the White Rose Grid. Both authors are very grateful to the Nordic Institute for Theoretical Physics (NORDITA), where this work was completed, as well as to the organisers of the NORDITA research program “Physics of Relativistic Flows” for hospitality and generous support.

REFERENCES

- Aloy M.A., Muller E., Abner J.M., Marti J.M., MacFadyen A.I., 2000, *ApJ*, 531, L119
- Ardeljan N.V., Bisnovatyi-Kogan G.S., Moiseenko S.G., 2005, *MNRAS*, 359, 333
- Bardeen J.M., Press W.H., Teukolsky S.A., 1972, *ApJ*, 178, 347
- Barkov M.V., Komissarov S.S., 2008a, *MNRAS*, 385, L28
- Barkov M.V., Komissarov S.S., 2008b, *AIPC*, 1085, 608
- Beck R., 2008, *AIPC*, 1085, 83
- Beck R., Krause M., 2005, *Astro. Nach.*, 326, 414
- Bezchastnov V.G., Haensel P., Kaminker A.D., Yakovlev D.G., 1997, *A&Ap*, 328, 409
- Bethe H.A., 1990, *Rev.Mod.Phys.*, 62, 801
- Birkel R., Aloy M.A., Janka H.Th., Miller E., 2007, *A&A*, 463, 51
- Bisnovatyi-Kogan G.S., 1970, *Astron.Zh.*, 47, 813 (*Soviet Astron.*, 1971, 14, 652)
- Bisnovatyi-Kogan G.S., Ruzmaikin A.A., 1974, *Ap&SS*, 28, 45
- Bisnovatyi-Kogan G.S., Tutukov A.V., 2004, *Astr. Rep.*, 48, 724
- Blandford R.D. and Znajek R.L., 1977, *MNRAS*, 179, 433
- Bloom J.S., Djorgovski S.G., Kulkarni S.R., Frail D.A., 1998, *ApJ*, 507, L25
- Brandenburg A., Nordlund A., Stein R.F., Torkelsson U., 1995, *ApJ*, 446, 741
- Braithwaite J., Spruit H.C., 2004, *Nature*, 431, 819
- Bucciantini N., Quataert E., Metzger B.D., Thompson T.A., Arons J., Del Zanna L., 2009, *MNRAS*, 391, 759B
- Burrows A., Dessart L., Livne E., Ott C.D., Murphy J., 2007, *ApJ*, 664, 416
- Burlon D., Ghirlanda G., Ghisellini G., Lazzati D., Nava L., Nardini M., Celotti A., 2008, *ApJ*, 685, L19
- Carpano S., Pollock A.M.T., Prestwich A., Crowther P., Wilms J., 2007, *A&A*, 466, L17
- Charbonneau P., MacGregor K.B., 2001, *ApJ*, 559, 1094.
- Chen W.-X., Beloborodov A.M., 2007, *ApJ*, 657, 383
- Cherepashchuk A.M., Mofat A.F.J., 1994, *ApJ*, 424, L53
- Chincarini G., Moretti A., Romano P., Falcone A.D., Morris D., 2007, *ApJ*, 671, 1903
- Clark J.S., Crowther P.A., *A&A*, 414, L45
- Crowther P.A., 2007, *ARA&A*, 45, 177
- Drenkhahn G., Spruit H. C., 2002, *A&A*, 391, 1141
- Donati J.F., Babel J., Harries T.J., Howarth I.D., Petit P., Semel M., 2002, *MNRAS*, 333, 55
- Fragos T., Willems B., Kalogera V., Ivanova N., Rockefeller G., Fryer C.L., Young P.A., 2009, *ApJ*, 697, 1057
- Fruchter A.S. et al., 2006, *Nature*, 441, 463
- Gualandris A., Colpi M., Zwart S.P., Possenti A., 2005, *ApJ*, 618, 845
- Guan X., Gammie C.F., 2009, *ApJ*, 559, 1094
- Heger A., Woosley S.E., Langer N., Spruit H.C., 2004, *IAUS*, 215, 591
- Heger A., Woosley S.E., Spruit H.C., 2005, *ApJ*, 626, 350
- Igumenshchev I., 2008, *ApJ*, 677, 317
- Ivanova L.N., Imshennik V.S., Nadezhin D.K., 1969, *Sci.Inf.Astr.Council.Acad.Sci*, 13,3
- Izzard R.G., Ramirez-Ruiz E., Tout C.A., 2004, *MNRAS*, 348, 1215
- Janiuk A., Proga D., 2008, *ApJ*, 675, 519
- Janiuk A., Moderski R., Proga D., 2009, *ApJ*, 687, 433
- Komissarov S.S., 1999, *MNRAS*, 303, 343
- Komissarov S.S., 2004, *MNRAS*, 350, 1431
- Komissarov S.S., Barkov M.V., 2007, *MNRAS*, 382, 1029
- Komissarov S.S., Barkov M.V., 2009, *MNRAS*, 397, 1153
- LeBlanc L.M., Wilson J.R., 1970, *ApJ*, 161, 541
- Lee H.K., Brown G.E., Wijers R.A.M.J., 2000, *ApJ*, 536, 416
- Lipunov V., Gorbvskoy E., 2007, *ApJ*, 665, L97
- Lipunov V., Gorbvskoy E., 2008, *MNRAS*, 383, 1397
- MacFadyen A.I., Woosley S.E., 1999, *ApJ*, 524, 262
- MacFadyen A.I., Woosley S.E., Heger A., 2001, *ApJ*, 550, 410
- McKinney J.C., 2006, *MNRAS*, 368, 1561
- Mészáros P., Rees M.J., 1997, *ApJ Lett.*, 482, L29
- Metzger B.D., Thompson T.A., & Quataert E., 2007, *ApJ*, 659, 561
- Moiseenko S.G., Bisnovatyi-Kogan G.S., Ardeljan N.V., 2006, *MNRAS*, 370, 501
- Perna R., Armitage P.J., Zhang B., 2006, *ApJ*, 636, L29
- Proga D., MacFadyen A.I., Armitage P.J., Begelman M.C., 2003, *ApJ*, 629, 397
- Plavec M., Krotochvile P., 1964, *BAICz*, 15, 165
- Podsiadlowski Ph., Mazzali P.A., Nomoto K., Lazzati D., Cappellaro E., 2004, *ApJ*, 607, L17
- Popham R., Woosley S.E., Fryer C., 1999, *ApJ*, 518, 356
- Prestwich A.H., Kilgard R., Crowther P.A., Carpano S., Pollock A.M.T., 2007, *ApJ*, 669, L21
- Rothstein D.M., Lovelace, R.V.E., 2008, *ApJ*, 677, 1221
- Schaerer D., Maeder A., 1992, *A&A*, 263, 129
- Schinder P.J., Schramm D.N., Wiita P.J., Margolis S.H., Tubbs D.L., 1987, *ApJ*, 313, 531.
- Schweickhardt J., Schmutz W., Stahl O., Szeifert Th., Wolf B., 1999, *A&A*, 347, 127
- Shakura N.I., Sunyaev R.A., 1973, *A&A*, 24, 337
- Shibata M., Shapiro S.L., 2002, *ApJ*, 572, L39
- Silverman J.M. & Filippenko A.V., 2008, *astro-ph/0802.2716*
- Sokolov et al., 2001, *A&A*, 372, 438
- Spruit H.C., Uzdensky D.A., 2005, *ApJ*, 629, 960
- Thompson T.A., Chang P., Quataert E., 2004, *ApJ*, 611, 380
- Thorne K.S., 1974, *ApJ*, 191, 507
- Timmes F.X., Swesty F.D., 2000, *ApJSS*, 126, 501

- Tutukov A.V. & Cherepashchuk, 2003, *Astronomy Reports*, 47, 386
 Tutukov A.V. & Cherepashchuk, 2003, *Astronomy Reports*, 48, 39
 Tutukov A.V., Fedorova A.V., 2007, *Astron. Rep.*, 51, 291
 Tutukov A.V., Yungelson L.R., 1979, *AcA*, 29, 665
 Usov V., 1992, *Nature*, 357, 472
 Uzdensky, D.A., 2007, *ApJ*, 671, 2139.
 Uzdensky D.A. & MacFadyen A.I., 2007, *ApJ*, 669, 546
 van Ballegoijen A.A., 1989, in *ASSL Vol. 156: Accretion Disks and Magnetic Fields in Astrophysics*, ed. G. Belvedere (Dordrecht: Kluwer Academic Publishers), 99
 van den Heuvel E.P.J. and Yoon S.C., 2007, *Astr.Sp.Sci*, 311, 177
 van Kerkwijk M.H., Charles P.A., Geballe T.R., King D.L., Miley G.K. et al, 1992, *Nature*, 355, 703
 Wang X.-Y., Meszaros P., 2007, *ApJ*, 670, 1247
 Woosley S.E., 1993, *ApJ*, 405, 273
 Woosley S.E., Baron E., 1992, *ApJ*, 391, 228
 Woosley S.E., Heger A., 2006, *ApJ*, 637, 914
 Yoon S.C., Langer N., 2005, *A&A*, 443, 643
 Yoon S.-C., Langer N., Norman C., 2006, *A&A*, 460, 199.
 Zalamea I., Beloborodov A.M., 2009, *AIPC*, 1133, 121
 Zhang B., 2007, *Chin.J.A&A*, 7(1), 1
 Zhang W., Fryer C.L., 2001, *ApJ*, 550, 357

APPENDIX A: EVOLUTION OF ANGULAR MOMENTUM AND MAGNETIC FIELD IN THE BETHE'S MODEL OF STELLAR COLLAPSE

The free fall model by Bethe (1990) approximates the kinematics of stellar collapse by the model

$$\frac{dR}{dt} = \begin{cases} 0 & \text{if } t \leq 0, \\ -(2GM(R)/R)^{-1/2} & \text{if } t > 0, \end{cases}$$

where R is the radius of collapsing shell and $M(R)$ is the mass inside this radius. Since $dM/dt = 0$, this equation is easily integrated

$$R_0(R, t) = R(1 + t/t_{ff}(R))^{2/3} = \text{const},$$

where $R_0 = R(0)$ and $t_{ff}(R) = \sqrt{2R^3/9GM(R)}$ is the local free fall time.

Given the initial distribution of angular momentum, $l_0 = \Omega(R_0 \sin \theta)^2$, the conservation of angular momentum yields

$$l(R, t) = l_0(R_0(R, T)) = \Omega_s(R \sin \theta)^2 (1 + t/t_{ff}(R))^{4/3}.$$

Similarly, the conservation of magnetic flux requires

$$\Psi(R, \theta, t) = \Psi_0(R_0(R, t), \theta).$$

For the uniform initial magnetic field,

$$\Psi_0(R_0, \theta) = \pi B_0 \sin^2 \theta R_0^2.$$

Thus,

$$\Psi(R, \theta, t) = \pi B_0 \sin^2 \theta R^2 (1 + t/t_{ff}(R))^{4/3}.$$

The poloidal magnetic field can be found via

$$B_p^i = \frac{1}{2\pi} e^{ij\varphi} \partial_j \Psi,$$

where e^{ijk} is the Levi-Civita tensor of space. This gives us

$$B^r = \frac{B_0 \sin \theta \cos \theta}{\sqrt{\gamma}} R^2 \left(1 + \frac{t}{t_{ff}(R)}\right)^{4/3} \quad (\text{A1})$$

and

$$B^\theta = \frac{B_0 \sin^2 \theta}{\sqrt{\gamma}} R \left(1 + \frac{t}{t_{ff}(R)}\right)^{1/3}, \quad (\text{A2})$$

where γ is the determinant of the metric tensor of space and the vector components are given in the non-normalised coordinate basis, $\partial/\partial x^i$. This approach has been used in Bisnovatyi-Kogan & Ruzmaikin (1974).